CORRECTED 12 APRIL 2017; SEE ERRATUM

SCIENCE TRANSLATIONAL MEDICINE | RESEARCH ARTICLE

CANCER

Integrated molecular analysis of tumor biopsies on sequential CTLA-4 and PD-1 blockade reveals markers of response and resistance

Whijae Roh,[1,2]* Pei-Ling Chen,[1,3]* Alexandre Reuben,[4]* Christine N. Spencer,[1] Peter A. Prieto,[4] John P. Miller,[5] Vancheswaran Gopalakrishnan,[4] Feng Wang,[1] Zachary A. Cooper,[1,4] Sangeetha M. Reddy,[6] Curtis Gumbs,[1] Latasha Little,[1] Qing Chang,[1] Wei-Shen Chen,[1,3] Khalida Wani,[7] Mariana Petaccia De Macedo,[7,8] Eveline Chen,[7] Jacob L. Austin-Breneman,[4] Hong Jiang,[4] Jason Roszik,[1,9] Michael T. Tetzlaff,[3] Michael A. Davies,[9] Jeffrey E. Gershenwald,[4] Hussein Tawbi,[9] Alexander J. Lazar,[4,7] Patrick Hwu,[9] Wen-Jen Hwu,[9] Adi Diab,[9] Isabella C. Glitza,[9] Sapna P. Patel,[9] Scott E. Woodman,[9] Rodabe N. Amaria,[9] Victor G. Prieto,[3] Jianhua Hu,[10] Padmanee Sharma,[11,12] James P. Allison,[11] Lynda Chin,[13] Jianhua Zhang,[14] Jennifer A. Wargo,[1,4†‡] P. Andrew Futreal[1†‡]

Immune checkpoint blockade produces clinical benefit in many patients. However, better biomarkers of response are still needed, and mechanisms of resistance remain incompletely understood. To address this, we recently studied a cohort of melanoma patients treated with sequential checkpoint blockade against cytotoxic T lymphocyte antigen–4 (CTLA-4) followed by programmed death receptor–1 (PD-1) and identified immune markers of response and resistance. Building on these studies, we performed deep molecular profiling including T cell receptor sequencing and whole-exome sequencing within the same cohort and demonstrated that a more clonal T cell repertoire was predictive of response to PD-1 but not CTLA-4 blockade. Analysis of CNAs identified a higher burden of copy number loss in nonresponders to CTLA-4 and PD-1 blockade and found that it was associated with decreased expression of genes in immune-related pathways. The effect of mutational load and burden of copy number loss on response was nonredundant, suggesting the potential utility of a combinatorial biomarker to optimize patient care with checkpoint blockade therapy.

INTRODUCTION

Immune checkpoint blockade represents a major advancement in cancer therapy for advanced melanoma. However, durable clinical responses are observed in only a minority of patients treated with single-agent cytotoxic T lymphocyte antigen–4 (CTLA-4) (*1*) or programmed death receptor–1 (PD-1) blockade (*2*, *3*). Although higher response rates are achieved when CTLA-4 and PD-1 inhibitors are administered concurrently, this regimen also has greatly increased toxicity (*3*, *4*). There is a clinical need to predict who will benefit from immunotherapy and to understand mechanisms of therapeutic resistance to improve patient management and outcomes. Recently, evidence has pointed to a role of tumor molecular features (such as mutational load) (*5*–*8*) and host immune infiltrates (*9*–*12*) in response to therapy, although complexities exist with the predictive power of these markers (*13*). Studies have also begun to uncover mechanisms of resistance, including expression of immune checkpoint molecules (*10*, *14*–*21*), insufficient infiltration of $CD8^+$ T cells (*9*, *10*), oncogenic pathways (*22*–*24*), transcriptomic resistance signatures (*25*), lack of sensitivity to interferon (IFN) signaling (*26*–*30*), defects in antigen processing and presentation (*11*, *30*–*32*), diversity and abundance of bacteria within the gut microbiome (*33*, *34*), and metabolism of cancer cells and T cells (*35*–*37*). However, additional insights are needed for a more comprehensive understanding of resistance.

To further refine both host and tumor genomic contributions to resistance to checkpoint blockade, we assembled a cohort of longitudinal tissue samples from metastatic melanoma patients treated with sequential immune checkpoint blockade (CTLA-4 blockade followed by PD-1 blockade at time of progression). We previously performed deep immune profiling studies on these samples (via immunohistochemistry and gene expression profiling) and identified immune biomarkers of response and mechanisms of therapeutic resistance (*38*). To complement these studies, we report here the results of in-depth molecular analysis [via whole-exome sequencing (WES) and T cell receptor (TCR) sequencing (TCR-seq)] of these longitudinal samples. These studies have identified putative genomic and molecular biomarkers of response and resistance to immune checkpoint blockade, demonstrating the complex interplay of host and tumor in treatment response.

[1]Department of Genomic Medicine, University of Texas MD Anderson Cancer Center, Houston, TX 77030, USA. [2]Cancer Biology Graduate Program, The University of Texas MD Anderson Cancer Center UTHealth Graduate School of Biomedical Sciences at Houston, Houston, TX 77030, USA. [3]Department of Pathology, University of Texas MD Anderson Cancer Center, Houston, TX 77030, USA. [4]Department of Surgical Oncology, University of Texas MD Anderson Cancer Center, Houston, TX 77030, USA. [5]Oncology Research for Biologics and Immunotherapy Translation, University of Texas MD Anderson Cancer Center, Houston, TX 77030, USA. [6]Division of Cancer Medicine, University of Texas MD Anderson Cancer Center, Houston, TX 77030, USA. [7]Department of Translational Molecular Pathology, University of Texas MD Anderson Cancer Center, Houston, TX 77030, USA. [8]Pathology Department, A.C.Camargo Cancer Center, São Paulo, SP-01509-010, Brazil. [9]Department of Melanoma Medical Oncology, University of Texas MD Anderson Cancer Center, Houston, TX 77030, USA. [10]Department of Biostatistics, University of Texas MD Anderson Cancer Center, Houston, TX 77030, USA. [11]Department of Immunology, University of Texas MD Anderson Cancer Center, Houston, TX 77030, USA. [12]Department of Genitourinary Medical Oncology, University of Texas MD Anderson Cancer Center, Houston, TX 77030, USA. [13]University of Texas System, Austin, TX 78701, USA. [14]Applied Cancer Science Institute, University of Texas MD Anderson Cancer Center, Houston, TX 77030, USA.
*These authors contributed equally to this work.
†Co-senior authors.
‡Corresponding author. Email: afutreal@mdanderson.org (P.A.F.); jwargo@mdanderson.org (J.A.W.)

RESULTS

T cell clonality predicts response to PD-1 blockade but not CTLA-4 blockade

We studied a cohort of 56 patients who were first treated with CTLA-4 blockade and then subsequently treated with PD-1 blockade at the time of progression, with longitudinal tumor samples collected as previously described (Fig. 1A and tables S1, A and B, and S2) (*38*) by performing WES and TCR-seq on DNA from available tumor samples (Fig. 1A, figs. S1 and S2, and table S3). Responders were defined as patients who had complete resolution or partial reduction in the size of tumors by computerized axial tomography (CAT) scan–based imaging (by at least 30%) or who had prolonged stable disease (for at least 6 months). Nonresponders were defined as patients who had tumor growth of at least 20% on CAT scan or had stable disease lasting less than 6 months. We first compared the mutation status of common melanoma driver genes (*39*, *40*) in pretreatment samples, also assessed IFN-γ pathway genes (given the importance of defects in IFN-γ signaling in resistance to immune checkpoint blockade) (*30*, *41*–*43*), and found no significant differences between responders and nonresponders to therapy with regard to somatic point mutations or indels (Fisher's exact test with a false discovery rate threshold of 0.05) (Fig. 1B and table S4). Next, we compared the frequency of human leukocyte antigen (HLA) somatic mutations (*44*) in pretreatment samples and found that HLA somatic mutations were found in only one pretreatment biopsy from a CTLA-4 blockade nonresponder (table S5). No particular genes were enriched for mutations in post–PD-1 blockade samples except *BRAF* (*V600E*) (five of six patients), potentially because of prolonged survival with interim *BRAF*-targeted therapy in three of five patients (Fig. 1B and table S1B).

In our cohort, we did not observe any statistically significant differences in mutational load or predicted neoantigen load in pretreatment samples from responders versus nonresponders to therapy by either CTLA-4 or PD-1 blockade (fig. S3, A and B, and table S6) (mutational load: $P = 0.597$ in pre–CTLA-4 blockade samples and $P = 0.885$ in pre–PD-1 blockade samples; neoantigen load: $P = 0.736$ in pre–CTLA-4 blockade samples and $P = 0.885$ in pre–PD-1 blockade samples), which is in contrast to published literature (*5*–*8*) and may be because of limited sample size. Furthermore, no significant differences were observed in intratumor heterogeneity (ITH), estimated as the number of clones per tumor, between responders and nonresponders to immune checkpoint blockade (fig. S4).

We next performed sequencing of the CDR3 variable region of the β chain of the TCR (TCR-seq) to understand the role of the T cell repertoire in response and resistance to checkpoint blockade (table S7). Although no significant differences were observed in TCR clonality when comparing responders to nonresponders in the context of CTLA-4 blockade at the pretreatment ($P = 0.96$) and on-treatment time points ($P = 0.2$) (Fig. 1C), an increase in clonality was noted in a subset of patients treated with CTLA-4 blockade (fig. S5A). Among eight patients with matched longitudinal tumor samples (pre–CTLA-4 and pre–PD-1; $n = 8$) available, all three PD-1 blockade responders showed an increase in TCR clonality on CTLA-4 blockade, whereas this was the case in only one of five nonresponders to PD-1 blockade (fig. S5A). One patient (patient 50) classified as a nonresponder in the context of the trial criteria, who demonstrated an increase in clonality, appeared to have some clinical benefit from treatment with PD-1 blockade, as he continued on PD-1 blockade therapy for a total of 24 doses and had no evidence of disease at the last follow-up. Higher TCR clonality was observed in responders to PD-1 blockade at both pretreatment ($P = 0.041$) and on-treatment ($P = 0.032$) time points (Fig. 1C).

Next, we sought to investigate the association between TCR clonality and immune activation in the tumor microenvironment. To do so, we first calculated the immune score from gene expression profiling data (*38*) in our cohort (table S8). The immune score was defined as the geometric mean of gene expression in selected genes, including cytolytic markers, HLA molecules, IFN-γ pathway, selected chemokines, and adhesion molecules related to tumor rejection in the context of the immunologic constant of rejection (table S9) (*45*, *46*). Although no association was observed between TCR clonality and immune scores in pre–CTLA-4 blockade samples, a significant positive correlation was observed between TCR clonality and immune scores in pre–PD-1 blockade samples ($P = 0.0018$; fig. S5B).

High copy number loss burden is associated with poor response to immune checkpoint blockade

Given the lack of clear differences in point mutation and indel status in driver genes between responders and nonresponders to CTLA-4 and PD-1 blockade, we then investigated whether copy number alterations (CNAs) may play a role in response and resistance to CTLA-4 and PD-1 blockade (table S10). With regard to specific genes, we did not find any significant association between copy number gain or loss status and response to therapy in pretreatment biopsies for either therapy (Fisher's exact test with a false discovery rate threshold of 0.05). Given a recent report demonstrating the impact of loss of HLA class I and β_2-microglobulin in resistance to cytolytic activity (*11*), we next examined the relevance of copy number loss in these genes within our cohort. Here, although we observed no significant loss of HLA class I genes, loss of β_2-microglobulin was detected in four nonresponders to CTLA-4 blockade (with focal copy number loss in two patients and arm-level copy number loss in two patients). Focal copy number loss of β_2-microglobulin was also observed in one pretreatment sample from a CTLA-4 blockade–naïve PD-1 blockade responder. To assess CNAs at the whole-genome sample level, we defined burden of CNAs as the total number of genes with copy number gain or loss per sample (table S2). On testing the association between burden of CNAs and response to therapy in pretreatment biopsies of patients on CTLA-4 or PD-1 blockade, we observed no significant differences in burden of copy number gain or loss ($P > 0.05$ for all comparisons) in the context of individual agent response (fig. S6). However, a trend toward higher burden of copy number loss was observed in pre–CTLA-4 blockade biopsies from CTLA-4 blockade responders compared to CTLA-4 blockade nonresponders, although statistical significance was not attained ($P = 0.077$).

We next investigated the burden of CNAs in pre–CTLA-4 blockade biopsies from patients who progressed on CTLA-4 blockade first and then progressed on PD-1 blockade, termed DNRs, because we hypothesized that the association between burden of CNAs and resistance might be stronger in patients with potentially more resistant phenotype (failure on both treatments) than in patients who failed a single agent. We observed no significant differences in burden of copy number gain but significantly higher burden of copy number loss in pre–CTLA-4 blockade biopsies from DNRs compared to pre–CTLA-4 blockade biopsies from CTLA-4 blockade responders ($P = 0.042$) (Fig. 2A and fig. S7). We noted a markedly higher burden of copy number loss in post–PD-1 blockade biopsies compared to pre–CTLA-4 blockade biopsies from CTLA-4 blockade responders ($P = 0.029$) (Fig. 2A and fig. S7). The burden of copy number loss was not correlated with mutational load at any time points studied (fig. S8), suggesting that the association is not readily attributable to decreased mutational burden.

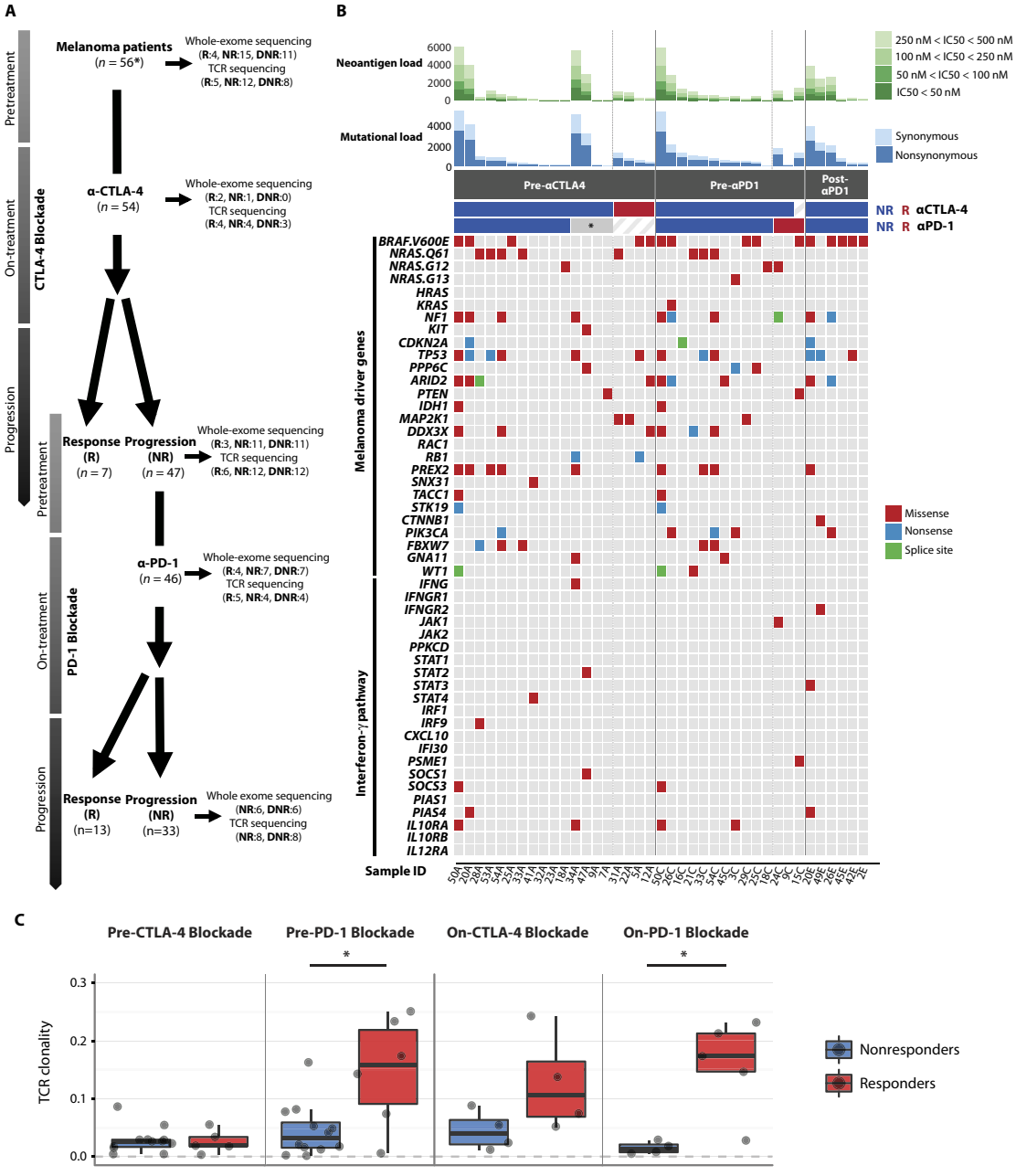

Fig. 1. Genomic landscape of serial tumor biopsies and genomic and immune correlates of treatment response. (**A**) Patients with metastatic melanoma were initially treated with CTLA-4 blockade ($n = 56$; asterisk indicates that 2 of the 56 patients were CTLA-4 blockade–naïve). Both responded to PD-1 blockade, and only pretreatment samples were available for WES and TCR-seq. Nonresponders (NRs) to CTLA-4 blockade ($n = 47$) were then treated with PD-1 blockade. Double nonresponders (DNRs) progressed on CTLA-4 blockade first and then progressed on PD-1 blockade. Serial tumor biopsies were collected at multiple time points (pretreatment, early on-treatment, and progression on CTLA-4 blockade and PD-1 blockade) when feasible. WES and TCR-seq were performed on these serial tumor biopsies. The numbers in parentheses indicate the number of samples available for responders (Rs) and nonresponders after quality control of WES and TCR-seq data. (**B**) For each sample (columns), genomic profiles (rows) were characterized. Column annotations represent biopsy time (pre–αCTLA-4, pre–CTLA-4 blockade samples; pre–αPD-1, pre–PD-1 blockade samples; post–αPD-1, post–PD-1 blockade samples) and response status (red, responders; blue, nonresponders; asterisk indicates failed CTLA-4 blockade but responded to PD-1 blockade) for each sample (sample ID denotes patient ID followed by biopsy time: A, pre–αCTLA-4; C, post–CTLA-4/pre–PD-1; E, post–PD-1). Mutational burden and neoantigen burden for each sample are shown at the top of the panel. Neoantigens were defined as having a median inhibitory concentration (IC_{50}) <500 nM. Color scale shows the range of IC_{50} from 500 to 50 nM. Synonymous (light) and nonsynonymous (dark) mutations are shown in different shades of blue. Additional genomic profiles included selected somatic point mutations and indels. No indels were found among melanoma driver genes. When multiple mutations were found in one gene, the following precedence rule was applied: nonsense mutation > frameshift indel > splice site mutation > missense mutation > in-frame indel. (**C**) Boxplots summarize TCR clonality by response status (blue, nonresponders; red, responders) in pre–CTLA-4 blockade samples, pre–PD-1 blockade samples, on–CTLA-4 blockade samples, and on–PD-1 blockade samples; median values (lines) and interquartile range (whiskers) are indicated. *P* values were calculated using two-sided Mann-Whitney *U* test ($P > 0.05$ for TCR clonality in pre–CTLA-4 blockade and on–CTLA-4 blockade samples, $P = 0.041$ for TCR clonality in pre–PD-1 blockade samples, and $P = 0.032$ for TCR clonality in on–PD-1 blockade samples).

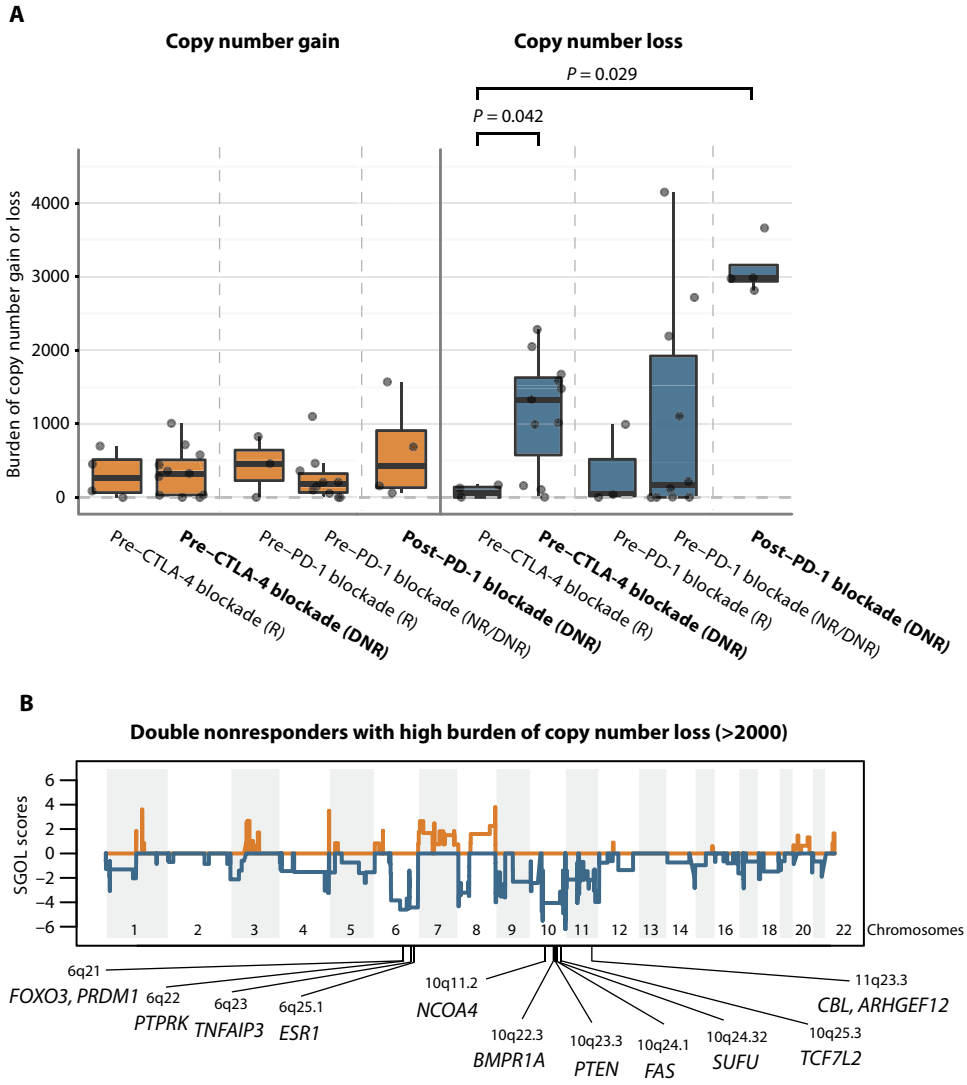

Fig. 2. Copy number loss as a potential resistance mechanism. (**A**) Boxplots summarize burden of copy number gain or loss in five groups of interest: responders to CTLA-4 blockade assessed before treatment, pre–CTLA-4 blockade DNRs, responders to PD-1 blockade assessed before treatment, pre–PD-1 blockade DNRs, and post–PD-1 blockade DNRs; median values (lines) and interquartile range (whiskers) are indicated. *P* values were calculated using two-sided Mann-Whitney *U* test ($P = 0.042$ for pre–CTLA-4 blockade responders versus DNRs, $P = 0.029$ for pre–CTLA-4 blockade responders versus post–PD-1 blockade DNRs, and $P > 0.05$ for all others). The pre–CTLA-4 blockade and post–PD-1 blockade DNR groups are highlighted in bold. (**B**) Segment gain or loss (SGOL) scores were calculated for each copy number segments as sum of $\log_2$ copy ratios (tumor/normal) of each copy number segment across all DNR samples with copy number loss burden higher than 2000 ($n = 9$). Higher positive SGOL scores indicate higher copy number gain of copy number segments, and lower negative SGOL scores indicate higher copy number loss of copy number segments. Tumor suppressor genes with recurrent copy number loss are indicated in chromosomes 6q, 10q, and 11q23.3.

To gain insight into mechanisms through which CNAs could influence response to therapy, we next investigated whether there were any recurrent regions of copy number loss in DNRs with high burden of copy number loss (>2000 genes with copy number loss). Recurrent copy number loss was observed at the arm level in chromosomes 6q and 10q, and recurrent focal copy number loss was observed in 8p23.3, 11p15.5, 11q23, 11q24, and 11q25 (Fig. 2B and table S11). In these regions with recurrent copy number loss, tumor suppressor genes were located in chromosomes 6q (*FOXO3*, *PRDM1*, *PTPRK*, *TNFAIP3*, and *ESR1*), 10q (*NCOA4*, *BMPR1A*, *PTEN*, *FAS*, *SUFU*, and *TCF7L2*), and 11q23.3 (*CBL* and *ARHGEF12*). These data suggest that the high burden of copy number loss in DNRs is associated with recurrent copy number loss in tumor suppressor genes located in chromosomes 6q, 10q, and 11q23.3.

An independent patient cohort shows copy number loss as a putative resistance mechanism

To investigate the impact of higher burden of copy number loss on resistance in another cohort of patients on immune checkpoint blockade, we obtained WES SAM files from 110 melanoma patients and RNA sequencing (RNA-seq) data from a subset of 42 melanoma patients (*7*) and reanalyzed the data using the same informatics pipeline and calling criteria. We then tested the association between the burden of CNAs (tables S12 and S13) and response to therapy in pretreatment biopsies on CTLA-4 blockade using the same response criteria (clinical benefit, long-term survival with no clinical benefit, and minimal or no clinical benefit), as previously described (*7*). Although the burden of copy number gain was not significantly associated with clinical benefit from CTLA-4 blockade, a lower burden of copy number loss was significantly associated with clinical benefit ($P = 0.016$) (Fig. 3A). As observed in our cohort, the burden of copy number loss once again did not correlate with mutational load (fig. S9). When examining the regions associated with recurrent copy number loss in the no clinical benefit subgroup, recurrent copy number loss was observed at arm level in chromosomes 9p and 10q, and recurrent focal copy number loss was observed in 4q35.2, 6q25, 6q27, and 11p15.5 (fig. S10 and table S14). Among these regions, tumor suppressor genes were observed in 6q25.1 (*ESR1*) and 10q (*NCOA4*, *BMPR1A*, *PTEN*, *FAS*, and *SUFU*), as observed within our cohort. Notably, no recurrent copy number loss was observed in any tumor suppressor gene in the clinical benefit and long-term survival subgroups.

Next, we investigated whether the recurrent region of copy number loss identified in our cohort (table S11) is also associated with CTLA-4 blockade resistance in this independent cohort (Van Allen cohort). To do so, we calculated the burden of copy number loss in this independent cohort as the total number of genes with copy number loss in the recurrent regions of copy number loss identified in our cohort. We observed a significantly higher burden of copy number loss in the minimal or no

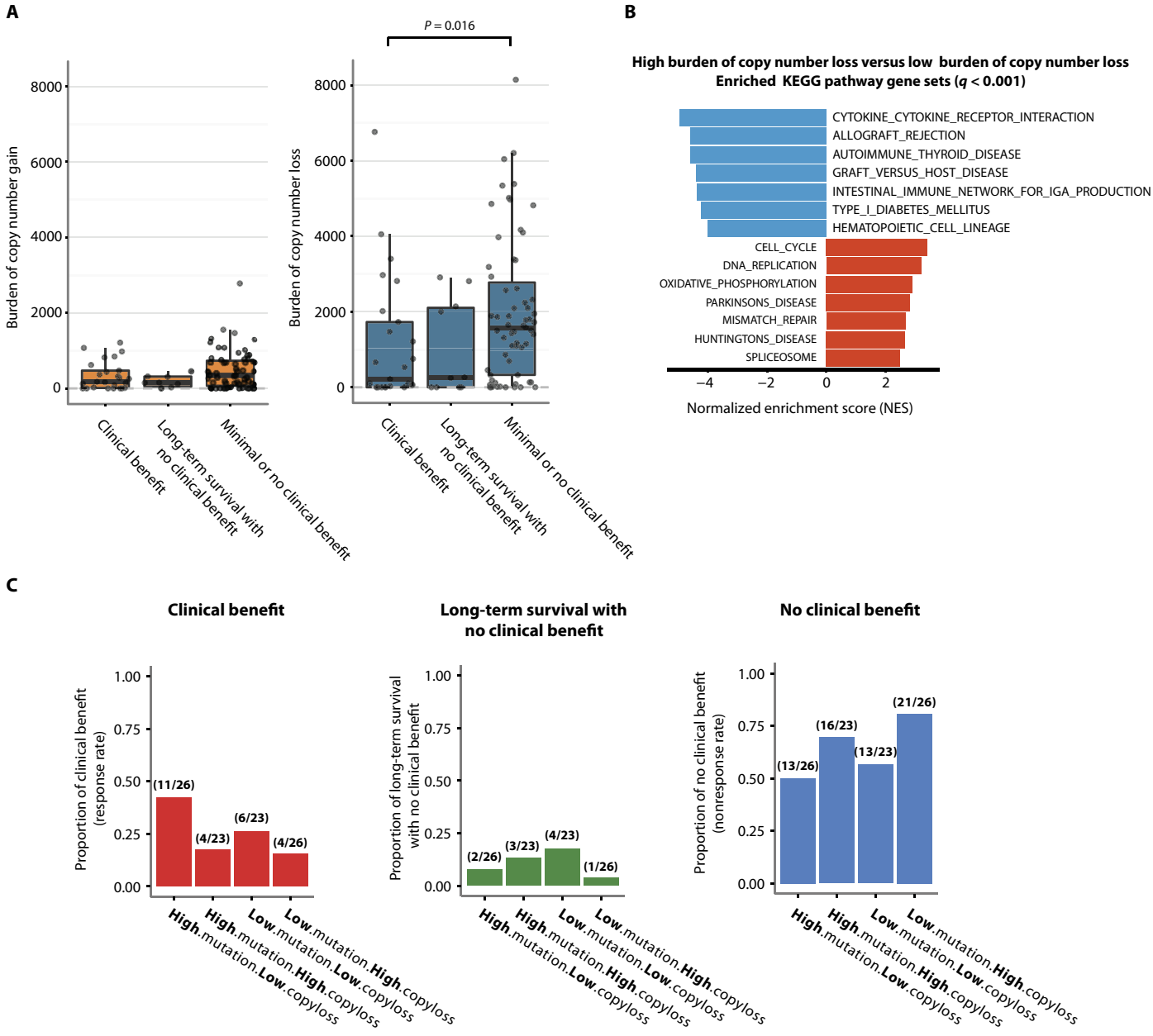

Fig. 3. Copy number loss as a potential resistance mechanism in an independent cohort. (**A**) Boxplots summarize burden of copy number gain or loss in three patient subgroups from the Van Allen cohort: clinical benefit, long-term survival with no clinical benefit, and minimal or no clinical benefit; median values (lines) and interquartile range (whiskers) are indicated. *P* values were calculated using two-sided Mann-Whitney *U* test ($P = 0.016$ for burden of copy number loss in clinical benefit versus minimal or no clinical benefit and $P > 0.05$ for all others). (**B**) Gene set enrichment analysis (GSEA) results show top enriched KEGG (Kyoto Encyclopedia of Genes and Genomes) pathways from down-regulated genes (blue bars) and up-regulated genes (red bars) in high burden of copy number loss group versus low burden of copy number loss group (false discovery rate–adjusted $P < 0.001$). (**C**) Proportions of patients with clinical benefit, long-term survival with no clinical benefit, and minimal or no clinical benefit were calculated within each of the four patient subgroups: high mutational load and low burden of copy number loss, high mutational load and high burden of copy number loss, low mutational load and low burden of copy number loss, and low mutational load and high burden of copy number loss. The numbers in parentheses indicate the number of patients with different levels of response (clinical benefit, long-term survival, and no clinical benefit) out of the total number of patients in each of the four patient subgroups.

clinical benefit groups compared to the clinical benefit group ($P = 0.0034$) (fig. S11). This result suggests that the recurrent regions of copy number loss in our cohort are also associated with CTLA-4 blockade resistance in this independent cohort.

We next sought to determine the relative contribution of copy number loss burden from chromosome 10 in CTLA-4 blockade resistance. We were specifically interested in copy number loss from chromosome 10 because a recent study (*47*) showed functional evidence that recurrent loss of the entire chromosome 10 can result in collective repression of multiple tumor suppressor genes. This is also consistent with the observation that chromosome 10 harbored the largest number of tumor suppressor genes with recurrent copy number loss in both our cohort

(Fig. 2B) and the independent cohort (fig. S10). The logistic regression model showed that the odds of resistance to CTLA-4 blockade were exp(1.504) = 4.5 [95% confidence interval (CI), 1.56 to 13] times greater in patients with high burden of copy number loss in chromosome 10 than in patients with low burden of copy number loss in chromosome 10 (table S15A), and the odds of resistance were exp(1.069) = 2.91 (95% CI, 1.07 to 7.89) times greater in patients with high burden of copy number loss outside chromosome 10 than in patients with low burden of copy number loss outside chromosome 10 (table S15B). Therefore, the relative contribution of copy number loss burden from chromosome 10 in CTLA-4 blockade resistance was higher than copy number loss burden outside chromosome 10. We further investigated the extent to which *PTEN* loss in chromosome 10 is associated with CTLA-4 blockade resistance (*24*). In our data, the odds of resistance were 5.58 times greater in patients with *PTEN* loss than in patients with no *PTEN* loss (95% CI, 1.19 to 26.20) (table S15C), suggesting that *PTEN* loss is likely to be one of the driver resistance mechanisms exploited by tumors with high burden of copy number loss on chromosome 10.

Integrated analysis reveals putative mechanisms through which CNAs may influence response to therapy

In addition to studying the influence of copy number loss on molecular features such as tumor suppressor genes, we sought to study the relationship of these alterations with the immune tumor microenvironment. To do so, we examined the correlation between burden of copy number loss and immune scores. Although we observed no correlation between the burden of copy number loss and immune scores in pre–CTLA-4 blockade biopsies in our cohort (correlation coefficient, −0.13; Spearman rank correlation, $P = 0.79$), a moderate negative correlation between the burden of copy number loss and immune scores calculated by ESTIMATE (*48*) was identified in the Van Allen cohort (correlation coefficient, −0.41; Spearman rank correlation, $P = 0.011$) (fig. S12A) (*7*). In pre–PD-1 blockade biopsies in our cohort, we also observed a negative correlation between the burden of copy number loss and immune scores (correlation coefficient, −0.63; Spearman rank correlation, $P = 0.091$) (fig. S12B), although this could not be investigated in post–PD-1 blockade biopsies because of sample size. Our immune scores and those calculated by ESTIMATE (table S16) showed a strong positive correlation (correlation coefficient, 0.91; Spearman rank correlation, $P < 2.2 \times 10^{-16}$) in the independent cohort (fig. S12C), suggesting concordance between immune scores.

We further sought to determine which pathways or gene ontologies (GOs) were enriched in up- or down-regulated genes at the mRNA expression level in the high burden of copy number loss groups ($n = 10$; mean, 4149; range, 2815 to 6764) versus the low burden of copy number loss groups ($n = 10$; mean, 0) within the Van Allen cohort. GSEA (*49*) showed that immune-related pathways were enriched among down-regulated genes, whereas cell cycle–related pathways were enriched among up-regulated genes (Fig. 3B, fig. S13A, and table S17, A to C). Similar results were found with GO terms (fig. S13B and table S17, A, D, and E). Collectively, these data suggest that high burden of copy number loss may be associated with down-regulation of immune-related pathways.

Mutational load and burden of copy number loss may allow better patient stratification for response than either correlate alone

Finally, we were interested in determining whether the effect of mutational load and burden of copy number loss on clinical response were nonredundant. Using the reanalyzed data from the Van Allen cohort, we first stratified patients into four subgroups based on mutational load (high or low) and burden of copy number loss (high or low) (fig. S14). Within each subgroup, we then calculated the proportion of patients with clinical benefit, long-term survival, and no clinical benefit (Fig. 3C). The proportion of patients with clinical benefit was higher in the subgroup of patients with high mutational load and low burden of copy number loss (11 of 26) compared to the subgroup of patients with low mutational load and high burden of copy number loss (4 of 26) ($P = 0.064$, Fisher's exact test). Similarly, the proportion of patients with no clinical benefit was significantly higher in the subgroup of patients with low mutational load and high burden of copy number loss (21 of 26) compared to the subgroup of patients with high mutational load and low burden of copy number loss (13 of 26) ($P = 0.04$, Fisher's exact test). We then performed a logistic regression on response status (clinical response or no clinical response) with the $\log_2$-transformed mutational load and $\log_2$-transformed burden of copy number loss as covariates and found an additive effect of mutational load (coefficient, 0.266; $z = 1.939$, $P = 0.053$) and burden of copy number loss (coefficient, −0.149; $z = -2.55$, $P = 0.011$) on clinical response (table S18). This suggests that the effects of mutational load and burden of copy number loss on clinical response are likely nonredundant. Collectively, the above-mentioned data demonstrate the potential utility of a combinatorial biomarker using mutational load and copy number loss burden.

DISCUSSION

Now, there is abundant evidence that both tumor-related (*5–8, 23, 24*) and host-related factors (*9–12*) can influence heterogeneous response and resistance to immune checkpoint blockade. Here, we report genomic characterization of tumors from a cohort of metastatic melanoma patients in the context of sequential immune checkpoint blockade. This study builds on our previous immune profiling of tumors within the same cohort of metastatic melanoma patients (*38*), allowing for a more integrated analysis in this particular cohort.

In tumor compartment–specific analyses, we observed a higher burden of copy number loss in nonresponders compared to responders on CTLA-4 blockade. This finding is in line with those in previous studies that have reported that the burden of CNAs increases in advanced melanoma and is implicated in melanoma progression (*50–53*). The association between burden of copy number loss and clinical response observed here suggests that melanoma progression may be associated with resistance to immune-mediated tumor control. Furthermore, investigation of the findings reported here in a first-line treatment setting will help delineate the value of these potential associations.

We also identified genomic regions of recurrent copy number loss in patients with high burden of copy number loss and determined that several tumor suppressor genes were located within these genomic regions. This suggests that loss of function in these tumor suppressor genes could potentially influence therapeutic resistance. In keeping with this suggestion, previous studies in preclinical models of melanoma with *PTEN* loss showed inhibition of T cell–mediated tumor killing and decrease in T cell trafficking into tumors (*24*). *PTEN* was one of the tumor suppressor genes with recurrent copy number loss from patients with high burden of copy number loss in this study as well. A correlation between copy number loss burden and down-regulation of immune-related gene expression was found, suggesting that there may be gene expression sequelae of extensive copy number loss, including *PTEN* loss. More extensive analyses on larger cohorts with matched WES

and RNA-seq data are needed to expand on these findings and develop an integrated expression/copy number evaluation approach to validate and potentially exploit the correlation observed here.

We also observed that the effects of low copy number loss burden and high mutational load on clinical response are nonredundant, suggesting the possibility of a combinatorial biomarker using copy number loss burden and mutational load. From a clinical perspective, the optimal cutoffs for high or low copy number loss burden and mutational load will need to be further validated whether they are to affect improved patient stratification in the clinical setting.

Our work also confirms previous reports that TCR clonality is correlated with response to PD-1 blockade (*10*). A combinatorial biomarker approach of TCR clonality and genomic correlates such as mutational load and copy number loss burden needs to be further tested in a large cohort with pre–PD-1 blockade biopsies available.

Additionally, we observed increased TCR clonality after CTLA-4 blockade treatment in all PD-1 blockade responders with paired pre–CTLA-4 and pre–PD-1 blockade biopsies available. Previous work has shown that TCR clonality at the pre–PD-1 time point was not significantly different ($P = 0.1604$) between PD-1 blockade responders treated with anti–CTLA-4 and PD-1 blockade responders naïve to anti–CTLA-4 (*10*). Therefore, CTLA-4 blockade treatment may increase TCR clonality to a level high enough to mediate response to subsequent PD-1 blockade in certain patients. This result suggests that responders to PD-1 blockade may derive clinical benefit from previous CTLA-4 blockade, substantiating the utility of sequential CTLA-4 and PD-1 blockade. From a clinical perspective, sequential CTLA-4 and PD-1 blockade treatment might be able to increase the number of patients with high baseline TCR clonality before PD-1 blockade compared with PD-1 blockade monotherapy.

What emerges from this and other works regarding immune checkpoint responder/nonresponder identification is a complex picture likely involving the interplay of tumor genomic characteristics, tumor modulation of the local microenvironment, and the extent of immune surveillance in the tumor milieu at the time of initiation of therapy. Furthermore, several intriguing questions emerge from this and other works. What is the effect of CTLA-4 blockade on the molecular profile of anti–PD-1 responders? Do the data reported hold true when applied to CTLA-4 blockade treatment–naïve patients? To what extent do the data emerging from melanoma studies apply to other tumor treatment contexts? There will likely be a need to develop integrated molecular phenotyping approaches to more accurately delineate responders/nonresponders and develop tractable predictive models for these promising therapies.

MATERIALS AND METHODS

Study design

Serial tumor biopsies were collected from patients with metastatic melanoma treated with CTLA-4 blockade and/or PD-1 blockade through an expanded access program for MK-3475 at the University of Texas (UT) MD Anderson Cancer Center. From serial tumor biopsies, we generated multidimensional profiling data (WES, TCR-seq, and NanoString gene expression profiling). Multidimensional profiling data were analyzed to identify genomic and immune correlates of treatment response and resistance mechanisms of immune checkpoint blockade.

Patient cohort and tumor samples

A cohort of 56 patients with metastatic melanoma were included in this study (*38*). These patients were treated at the UT MD Anderson Cancer Center between October 2011 and March 2015, and tumor samples were collected with appropriate written informed consent and analyzed (IRB LAB00-063, LAB03-0320, 2012-0846, PA13-0291, and PA12-0305). All tumor measurements were performed by a physician formally trained in tumor metrics, specifically RECIST 1.1, because it applies to the cohort. All metrics used computerized axial tomography scan imaging of measurable lesions (total of five lesions and maximum of two per organ) that met measurability based on strict RECIST 1.1 criteria (>10-mm-long axis per target lesion or >15-mm-short axis for target lymph nodes). The sums of these respective diameters were compared to the sum at baseline. According to RECIST 1.1 criteria, a lymph node with <10-mm-short axis was considered nonpathologic. As such, patients were first defined as those having either (i) a complete response [disappearance of all target lesions, reduction in any pathological lymph nodes (whether target or not) in short axis to <10 mm, and the appearance of no new lesions], (ii) a partial response (at least a 30% decrease in the sum of diameters of target lesions, no PD in nontarget lesions, and the appearance of no new lesions), (iii) progressive disease (at least a 20% increase in the sum of diameters of target lesions, taking the smallest sum or baseline as reference, with a minimum absolute increase of 5 mm, and/or the development of any new lesions), or (iii) stable disease [neither sufficient decrease to designate complete response/partial response nor increase to qualify as progressive disease (again using the smallest sum of appropriate diameters as a reference)]. All image responses were vetted with ≥2 serial images over a ≥6-month interval between baseline and assignment of response. RECIST 1.1 quantification of response was then used to assign patient designation as responder (complete response, partial response, or stable disease for ≥6 months) or nonresponder (progressive disease or stable disease with <6-month duration). All specimens were excisional biopsies or resection specimens. Tumor samples were assessed by two pathologists for adequate tumor tissue for WES (table S2).

Sample processing

After fixation and mounting, 5 to 10 slices with 5-μm thickness were obtained from formalin-fixed, paraffin-embedded (FFPE) tumor blocks. Tumor-enriched tissue was macrodissected, and xylene (EMD Millipore) was used for deparaffinization, followed by two ethanol washes. Reagents from the Qiagen QIAamp DNA FFPE Tissue Kit (#56404) were used in conjunction with an overnight incubation at 55°C to complete tissue lysis. Next, samples were incubated at 90°C for 1 hour to reverse formaldehyde modification of nucleic acids. After isolation by QIAamp MinElute column, variable amounts of buffer ATE were added to each column to elute the DNA. Germline DNA was obtained from peripheral blood mononuclear cells.

Whole-exome sequencing

The initial genomic DNA input into the shearing step was 250 ng in 55 μl of low tris-EDTA buffer. Forked Illumina paired-end adapters with random eight–base pair indexes were used for adapter ligation. All reagents used for end repair, A-base addition, adapter ligation, and library enrichment polymerase chain reaction (PCR) were from the KAPA Hyper Prep Kit (#KK8504). Unligated adapter and/or adapter-dimer molecules were removed from the libraries before cluster generation using solid-phase reverse immobilization bead cleanup. The elution volume after postligation cleanup was 25 μl. Library construction was performed following the manufacturer's instructions. Sample concentrations were measured after library construction using the Agilent Bioanalyzer. Each hybridization reaction contained 650 to

750 ng of the prepared library in a volume of 3.4 μl. Samples were lyophilized and reconstituted to bring the final concentration to 221 ng/μl. After reconstitution, the Agilent SureSelectXT Target Enrichment (#5190-8646) protocol was followed according to the manufacturer's guidelines. The libraries were then normalized to equal concentrations using an Eppendorf Mastercycler EP Gradient instrument and pooled to equimolar amounts on the Agilent Bravo B platform. Library pools were quantified using the KAPA Library Quantification Kit (#KK4824).

On the basis of quantitative PCR quantification, libraries were then brought to 2 nM and denatured using 0.2 N NaOH. After denaturation, libraries were diluted to 14 to 20 pM using Illumina hybridization buffer. Next, cluster amplification was performed on denatured templates according to the manufacturer's guidelines (Illumina), HiSeq v3 cluster chemistry and flow cells, as well as Illumina's Multiplexing Sequencing Primer Kit. The pools were then added to flow cells using the cBot System, sequenced using the HiSeq 2000/2500 v3 sequencing-by-synthesis method, and then analyzed using RTA v.1.13 or later. Each pool of whole-exome libraries was subjected to paired 76–base pair runs. An eight–base pair index-sequencing read was used to meet coverage and to demultiplex the pooled samples. The mean coverage for exome data was 177× in tumors and 91× in germ line. Mean sequencing coverage and tumor purities were similar across groups, with the exception of on-treatment biopsies given the presence of lower tumor content and enriched immune infiltrates (fig. S2). Therefore, WES data from on-treatment samples were excluded from downstream analysis.

Mutation calling and ITH analysis

Exome sequencing data were processed using Saturn V, the next-generation sequencing data processing and analysis pipeline developed and maintained by the bioinformatics group of the Institute for Applied Cancer Science and Department of Genomic Medicine at the UT MD Anderson Cancer Center. BCL files (raw output of Illumina HiSeq) were processed using Illumina CASAVA (Consensus Assessment of Sequence and Variation) software (v1.8.2) for demultiplexing/conversion to FASTQ format. The FASTQ files were then aligned to the hg19 human genome build using BWA (v0.7.5) (*54*). The aligned BAM files were subjected to mark duplication, realignment, and recalibration using the Picard tool and GATK software tools (*55*–*57*). The BAM files were then used for downstream analysis. MuTect (v1.1.4) (*58*) was applied to identify somatic point mutations, and Pindel (v0.2.4) (*59*) was applied to identify small insertions and deletions. Somatic mutations in HLA genes were called by POLYSOLVER (v1.0) (*44*). EXPANDS (v1.6.1) (*60*) and SciClone (v1.0.7) (*61*) were applied with only loss of heterozygosity–free regions to estimate the number of clones per tumor.

Neoantigen prediction

HLA class I neoepitopes were predicted for each patient as previously described (*62*). Briefly, patient HLA-A, HLA-B, and HLA-C variants were identified using ATHLATES (v2014_04_26) (*63*). Next, all possible 9- to 11-mer peptides flanking a nonsynonymous exonic mutation were generated computationally, and binding affinity was predicted on the basis of patient HLA and compared to that of the wild-type peptide counterpart using NetMHCpan (v2.8) algorithm (*64*). Mutated peptides with predicted IC_{50} <500 nM were considered as predicted neoantigens. The Cancer Genome Atlas melanoma (*40*) gene expression data were used to further filter out predicted neoantigens with mean gene expression values below 5 [mean RSEM <5].

CNA analysis

Sequenza (v2.1.2) (*65*) was applied to obtain copy number segments of $\log_2$ copy ratios (tumor/normal) for each tumor sample. R package "CNTools" (v1.24.0) (*66*) was used to identify copy number gain ($\log_2$ copy ratios > $\log_2$1.5) or loss ($\log_2$ copy ratios < $-\log_2$1.5) at the gene level. The burden of copy number gain or loss was then calculated as the total number of genes with copy number gain or loss per sample. For recurrent CNA analysis, R package "cghMCR" (v1.26.0) (*67*) was applied to $\log_2$ copy ratios (tumor/normal) obtained from "exomecn" (in-house copy number caller). SGOL scores of copy number segments or genes were calculated as sum of $\log_2$ copy ratios of each copy number segment or gene across all samples within a group of interest. Copy number segments with both copy number gain and copy number loss present within a group were excluded. We identified genomic regions of recurrent CNAs [minimum common regions (MCRs)] using cghMCR function with the following parameters: gapAllowed, 500; alteredLow, $-\log_2(1.5)$; alteredHigh, $\log_2(1.5)$; recurrence, 60; spanLimit, 2+e+07; thresholdType, "value" (recurrent copy number loss was defined as copy number loss observed in more than 60% of samples in a group of interest). Tumor suppressor genes annotated in recurrent copy number loss plots were obtained as cancer genes present in both the COSMIC (v77) (*68*) and TSGene (*69*) databases. Four samples were excluded from analysis because of unusable copy number profiles (45C, 19D, 45E, and 20E).

TCR-seq and clonality analysis

TCR-seq of the CDR3 variable region of the β chain was performed by ImmunoSeq hsTCRB Kit as described previously (Adaptive Biotechnologies) (*70*, *71*). Briefly, DNA was extracted from FFPE tumor tissues, and CDR3 regions were amplified before sequencing by MiSeq 150× (Illumina). Data were then transferred to Adaptive Technologies for deconvolution of CDR3 β sequences. For each sample, Shannon entropy and TCR clonality were calculated using the ImmunoSeq Analyzer (*10*).

NanoString gene expression profiling

NanoString was performed using a custom codeset of 795 genes as previously described (*38*). Briefly, RNA was extracted using the RNeasy Mini Kit (Qiagen) from FFPE blocks, after initial confirmation of tumor presence and content by two pathologists using hematoxylin and eosin. For gene expression studies, 1 μg of RNA was used per sample. Hybridization was performed for 16 to 18 hours at 65°C, and samples were loaded onto the nCounter Prep Station for binding and washing before scanning and capture of 600 fields using the nCounter. Preprocessing of NanoString data was performed as previously described (*38*). Immune scores were calculated as geometric mean of gene expression of cytolytic markers (*GZMA*, *GZMB*, *PRF1*, and *GNLY*), HLA molecules (*HLA-A*, *HLA-B*, *HLA-C*, *HLA-E*, *HLA-F*, *HLA-G*, *HLA-H*, *HLA-DMA*, *HLA-DMB*, *HLA-DOA*, *HLA-DOB*, *HLA-DPA1*, *HLA-DPB1*, *HLA-DQA1*, *HLA-DQA2*, *HLA-DQB1*, *HLA-DRA*, and *HLA-DRB1*), IFN-γ pathway genes (*IFNG*, *IFNGR1*, *IFNGR2*, *IRF1*, *STAT1*, and *PSMB9*), chemokines (*CCR5*, *CCL3*, *CCL4*, *CCL5*, *CXCL9*, *CXCL10*, and *CXCL11*), and adhesion molecules (*ICAM1*, *ICAM2*, *ICAM3*, *ICAM4*, *ICAM5*, and *VCAM1*).

Independent (Van Allen) cohort analysis

Mutational load was obtained from nonsynonymous mutational load in a previous study (*7*). WES data (SAM files) from 110 melanoma patients and RNA-seq data from 42 patients (FASTQ files) were downloaded

through the dbGaP (accession number phs000452.v2.p1). CNAs were identified from the same computational pipeline as described above. For the Van Allen cohort, recurrent copy number loss was defined as copy number loss observed in more than 40% of samples in a group of interest. Twelve samples were excluded from analysis because of unusable copy number profiles (Pat06, Pat73, Pat78, Pat81, Pat92, Pat106, Pat121, Pat132, Pat165, Pat166, Pat171, and Pat175). In the minimal or no clinical benefit group, samples with low burden of copy number loss (<100) were excluded from recurrent CNA analysis. The relatively low cutoff of 100 was chosen to capture most of the recurrent events. For RNA-seq analysis, all the RNA-seq samples were first aligned to the human reference genome (hg19 and GRCh37.75) with Bowtie2 (v2.2.5). RSEM (v1.2.12) was used to quantify transcript expression at the gene level in fragments per kilobase of transcript per million mapped reads (FPKM). Immune scores for the independent cohort were calculated by ESTIMATE (*48*). eBayes-moderated *t* test was performed to compare the high burden of copy number loss ($n = 10$) and low burden of copy number loss ($n = 10$) groups. Rank metric was then calculated as the sign of $\log_2$ fold changes multiplied by inverse of *P* values. GSEA (*49*) was performed on the rank metric–sorted list of genes (table S17A).

Statistical analysis

Statistical analyses were performed using R 3.2.2. Statistical tests included two-sided Fisher's exact tests and two-sided Mann-Whitney *U* tests.

SUPPLEMENTARY MATERIALS

www.sciencetranslationalmedicine.org/cgi/content/full/9/379/eaah3560/DC1

Fig. S1. Workflow diagram of multidimensional profiling analysis.
Fig. S2. Distribution of sequencing coverage and tumor purities across samples.
Fig. S3. Mutational load, neoantigen load, and clinical response.
Fig. S4. ITH and clinical response.
Fig. S5. The effects of previous CTLA-4 blockade exposure on the baseline TCR clonality of pre–PD-1 blockade samples.
Fig. S6. Burden of CNAs in responders versus nonresponders.
Fig. S7. Copy number profiles of responders and DNRs.
Fig. S8. Correlation between burden of copy number loss and mutational load.
Fig. S9. Correlation between burden of copy number loss and mutational load in the Van Allen cohort.
Fig. S10. SGOL scores in three patient subgroups from the Van Allen cohort.
Fig. S11. Burden of recurrent CNAs in patients from the Van Allen cohort.
Fig. S12. Correlation between burden of copy number loss and immune scores.
Fig. S13. Up- and down-regulated pathways in patients with high copy number loss versus low copy number loss in the Van Allen cohort.
Fig. S14. Patient stratification based on mutational load and burden of copy number loss in the Van Allen cohort.
Table S1. Clinical and demographic characteristics of patient cohort.
Table S2. Sample information, tumor purity, mutational load, neoantigen load, number of clones per tumor, and burden of CNAs.
Table S3. Summary measure of the data across clinical subgroups.
Table S4. List of somatic point mutations and indels.
Table S5. List of HLA somatic mutations.
Table S6. List of neoantigens and predicted major histocompatibility complex binding affinity.
Table S7. TCR clonality.
Table S8. Log_2-transformed NanoString normalized count data in our cohort.
Table S9. Immune scores (NanoString) in our cohort.
Table S10. Log_2 copy number ratio segment file by Sequenza in our cohort.
Table S11. Recurrent CNAs in DNRs with copy number loss burden higher than 2000.
Table S12. Log_2 copy number ratio segment file by Sequenza in the Van Allen cohort.
Table S13. Burden of CNAs in the Van Allen cohort.
Table S14. Recurrent CNAs in the Van Allen cohort.
Table S15. Relative contribution of copy number loss burden on chromosome 10 in CTLA-4 blockade resistance.
Table S16. Immune scores (RNA-seq) in the Van Allen cohort.
Table S17. Preranked gene list for GSEA, KEGG pathway, and GO analysis in the Van Allen cohort.
Table S18. Additive effects of high mutational load and low burden of copy number loss on response to CTLA-4 blockade.

REFERENCES AND NOTES

1. D. Schadendorf, F. S. Hodi, C. Robert, J. S. Weber, K. Margolin, O. Hamid, D. Patt, T.-T. Chen, D. M. Berman, J. D. Wolchok, Pooled analysis of long-term survival data from phase II and phase III trials of ipilimumab in unresectable or metastatic melanoma. *J. Clin. Oncol.* **33**, 1889–1894 (2015).
2. S. L. Topalian, F. S. Hodi, J. R. Brahmer, S. N. Gettinger, D. C. Smith, D. F. McDermott, J. D. Powderly, R. D. Carvajal, J. A. Sosman, M. B. Atkins, Safety, activity, and immune correlates of anti–PD-1 antibody in cancer. *N. Engl. J. Med.* **366**, 2443–2454 (2012).
3. J. Larkin, V. Chiarion-Sileni, R. Gonzalez, J. J. Grob, C. L. Cowey, C. D. Lao, D. Schadendorf, R. Dummer, M. Smylie, P. Rutkowski, P. F. Ferrucci, A. Hill, J. Wagstaff, M. S. Carlino, J. B. Haanen, M. Maio, I. Marquez-Rodas, G. A. McArthur, P. A. Ascierto, G. V. Long, M. K. Callahan, M. A. Postow, K. Grossmann, M. Sznol, B. Dreno, L. Bastholt, A. Yang, L. M. Rollin, C. Horak, F. S. Hodi, J. D. Wolchok, Combined nivolumab and ipilimumab or monotherapy in untreated melanoma. *N. Engl. J. Med.* **373**, 23–34 (2015).
4. J. D. Wolchok, H. Kluger, M. K. Callahan, M. A. Postow, N. A. Rizvi, A. M. Lesokhin, N. H. Segal, C. E. Ariyan, R.-A. Gordon, K. Reed, M. M. Burke, A. Caldwell, S. A. Kronenberg, B. U. Agunwamba, X. Zhang, I. Lowy, H. D. Inzunza, W. Feely, C. E. Horak, Q. Hong, A. J. Korman, J. M. Wigginton, A. Gupta, M. Sznol, Nivolumab plus ipilimumab in advanced melanoma. *N. Engl. J. Med.* **369**, 122–133 (2013).
5. A. Snyder, V. Makarov, T. Merghoub, J. Yuan, J. M. Zaretsky, A. Desrichard, L. A. Walsh, M. A. Postow, P. Wong, T. S. Ho, T. J. Hollmann, C. Bruggeman, K. Kannan, Y. Li, C. Elipenahli, C. Liu, C. T. Harbison, L. Wang, A. Ribas, J. D. Wolchok, T. A. Chan, Genetic basis for clinical response to CTLA-4 blockade in melanoma. *N. Engl. J. Med.* **371**, 2189–2199 (2014).
6. N. A. Rizvi, M. D. Hellmann, A. Snyder, P. Kvistborg, V. Makarov, J. J. Havel, W. Lee, J. Yuan, P. Wong, T. S. Ho, Mutational landscape determines sensitivity to PD-1 blockade in non–small cell lung cancer. *Science* **348**, 124–128 (2015).
7. E. M. Van Allen, D. Miao, B. Schilling, S. A. Shukla, C. Blank, L. Zimmer, A. Sucker, U. Hillen, M. H. G. Foppen, S. M. Goldinger, J. Utikal, J. C. Hassel, B. Weide, K. C. Kaehler, C. Loquai, P. Mohr, R. Gutzmer, R. Dummer, S. Gabriel, C. J. Wu, D. Schadendorf, L. A. Garraway, Genomic correlates of response to CTLA-4 blockade in metastatic melanoma. *Science* **350**, 207–211 (2015).
8. D. T. Le, J. N. Uram, H. Wang, B. R. Bartlett, H. Kemberling, A. D. Eyring, A. D. Skora, B. S. Luber, N. S. Azad, D. Laheru, B. Biedrzycki, R. C. Donehower, A. Zaheer, G. A. Fisher, T. S. Crocenzi, J. J. Lee, S. M. Duffy, R. M. Goldberg, A. de la Chapelle, M. Koshiji, F. Bhaijee, T. Huebner, R. H. Hruban, L. D. Wood, N. Cuka, D. M. Pardoll, N. Papadopoulos, K. W. Kinzler, S. Zhou, T. C. Cornish, J. M. Taube, R. A. Anders, J. R. Eshleman, B. Vogelstein, L. A. Diaz Jr., PD-1 blockade in tumors with mismatch-repair deficiency. *N. Engl. J. Med.* **372**, 2509–2520 (2015).
9. O. Hamid, C. Robert, A. Daud, F. S. Hodi, W.-J. Hwu, R. Kefford, J. D. Wolchok, P. Hersey, R. W. Joseph, J. S. Weber, R. Dronca, T. C. Gangadhar, A. Patnaik, H. Zarour, A. M. Joshua, K. Gergich, J. Elassaiss-Schaap, A. Algazi, C. Mateus, P. Boasberg, P. C. Tumeh, B. Chmielowski, S. W. Ebbinghaus, X. N. Li, S. P. Kang, A. Ribas, Safety and tumor responses with lambrolizumab (anti-PD-1) in melanoma. *N. Engl. J. Med.* **369**, 134–144 (2013).
10. P. C. Tumeh, C. L. Harview, J. H. Yearley, I. P. Shintaku, E. J. M. Taylor, L. Robert, B. Chmielowski, M. Spasic, G. Henry, V. Ciobanu, A. N. West, M. Carmona, C. Kivork, E. Seja, G. Cherry, A. J. Gutierrez, T. R. Grogan, C. Mateus, G. Tomasic, J. A. Glaspy, R. O. Emerson, H. Robins, R. H. Pierce, D. A. Elashoff, C. Robert, A. Ribas, PD-1 blockade induces responses by inhibiting adaptive immune resistance. *Nature* **515**, 568–571 (2014).
11. M. S. Rooney, S. A. Shukla, C. J. Wu, G. Getz, N. Hacohen, Molecular and genetic properties of tumors associated with local immune cytolytic activity. *Cell* **160**, 48–61 (2015).
12. M. Angelova, P. Charoentong, H. Hackl, M. L. Fischer, R. Snajder, A. M. Krogsdam, M. J. Waldner, G. Bindea, B. Mlecnik, J. Galon, Z. Trajanoski, Characterization of the immunophenotypes and antigenomes of colorectal cancers reveals distinct tumor escape mechanisms and novel targets for immunotherapy. *Genome Biol.* **16**, 64 (2015).
13. T. N. Schumacher, C. Kesmir, M. M. van Buuren, Biomarkers in cancer immunotherapy. *Cancer Cell* **27**, 12–14 (2015).
14. J. Matsuzaki, S. Gnjatic, P. Mhawech-Fauceglia, A. Beck, A. Miller, T. Tsuji, C. Eppolito, F. Qian, S. Lele, P. Shrikant, L. J. Old, K. Odunsi, Tumor-infiltrating NY-ESO-1–specific $CD8^+$ T cells are negatively regulated by LAG-3 and PD-1 in human ovarian cancer. *Proc. Natl. Acad. Sci. U.S.A.* **107**, 7875–7880 (2010).
15. K. Sakuishi, L. Apetoh, J. M. Sullivan, B. R. Blazar, V. K. Kuchroo, A. C. Anderson, Targeting Tim-3 and PD-1 pathways to reverse T cell exhaustion and restore anti-tumor immunity. *J. Exp. Med.* **207**, 2187–2194 (2010).
16. H. Li, K. Wu, K. Tao, L. Chen, Q. Zheng, X. Lu, J. Liu, L. Shi, C. Liu, G. Wang, W. Zou, Tim-3/galectin-9 signaling pathway mediates T-cell dysfunction and predicts poor prognosis in

patients with hepatitis B virus-associated hepatocellular carcinoma. *Hepatology* **56**, 1342–1351 (2012).
17. S.-R. Woo, M. E. Turnis, M. V. Goldberg, J. Bankoti, M. Selby, C. J. Nirschl, M. L. Bettini, D. M. Gravano, P. Vogel, C. L. Liu, S. Tangsombatvisit, J. F. Grosso, G. Netto, M. P. Smeltzer, A. Chaux, P. J. Utz, C. J. Workman, D. M. Pardoll, A. J. Korman, C. G. Drake, D. A. A. Vignali, Immune inhibitory molecules LAG-3 and PD-1 synergistically regulate T-cell function to promote tumoral immune escape. *Cancer Res.* **72**, 917–927 (2012).
18. T. Powles, J. P. Eder, G. D. Fine, F. S. Braiteh, Y. Loriot, C. Cruz, J. Bellmunt, H. A. Burris, D. P. Petrylak, S.-l. Teng, X. Shen, Z. Boyd, P. S. Hegde, D. S. Chen, N. J. Vogelzang, MPDL3280A (anti-PD-L1) treatment leads to clinical activity in metastatic bladder cancer. *Nature* **515**, 558–562 (2014).
19. R. S. Herbst, J.-C. Soria, M. Kowanetz, G. D. Fine, O. Hamid, M. S. Gordon, J. A. Sosman, D. F. McDermott, J. D. Powderly, S. N. Gettinger, H. E. K. Kohrt, L. Horn, D. P. Lawrence, S. Rost, M. Leabman, Y. Xiao, A. Mokatrin, H. Koeppen, P. S. Hegde, I. Mellman, D. S. Chen, F. S. Hodi, Predictive correlates of response to the anti-PD-L1 antibody MPDL3280A in cancer patients. *Nature* **515**, 563–567 (2014).
20. R. J. Johnston, L. Comps-Agrar, J. Hackney, X. Yu, M. Huseni, Y. Yang, S. Park, V. Javinal, H. Chiu, B. Irving, D. L. Eaton, J. L. Grogan, The immunoreceptor TIGIT regulates antitumor and antiviral $CD8^+$ T cell effector function. *Cancer Cell* **26**, 923–937 (2014).
21. J.-M. Chauvin, O. Pagliano, J. Fourcade, Z. Sun, H. Wang, C. Sander, J. M. Kirkwood, T.-h. T. Chen, M. Maurer, A. J. Korman, H. M. Zarour, TIGIT and PD-1 impair tumor antigen-specific $CD8^+$ T cells in melanoma patients. *J. Clin. Invest.* **125**, 2046–2058 (2015).
22. H. Sumimoto, F. Imabayashi, T. Iwata, Y. Kawakami, The BRAF–MAPK signaling pathway is essential for cancer-immune evasion in human melanoma cells. *J. Exp. Med.* **203**, 1651–1656 (2006).
23. S. Spranger, R. Bao, T. F. Gajewski, Melanoma-intrinsic β-catenin signalling prevents anti-tumour immunity. *Nature* **523**, 231–235 (2015).
24. W. Peng, J. Q. Chen, C. Liu, S. Malu, C. Creasy, M. T. Tetzlaff, C. Xu, J. A. McKenzie, C. Zhang, X. Liang, L. J. Williams, W. Deng, G. Chen, R. Mbofung, A. J. Lazar, C. A. Torres-Cabala, Z. A. Cooper, P.-L. Chen, T. N. Tieu, S. Spranger, X. Yu, C. Bernatchez, M.-A. Forget, C. Haymaker, R. Amaria, J. L. McQuade, I. C. Glitza, T. Cascone, H. S. Li, L. N. Kwong, T. P. Heffernan, J. Hu, R. L. Bassett Jr., M. W. Bosenberg, S. E. Woodman, W. W. Overwijk, G. Lizée, J. Roszik, T. F. Gajewski, J. A. Wargo, J. E. Gershenwald, L. Radvanyi, M. A. Davies, P. Hwu, Loss of PTEN promotes resistance to T cell–mediated immunotherapy. *Cancer Discov.* **6**, 202–216 (2016).
25. W. Hugo, J. M. Zaretsky, L. Sun, C. Song, B. H. Moreno, S. Hu-Lieskovan, B. Berent-Maoz, J. Pang, B. Chmielowski, G. Cherry, E. Seja, S. Lomeli, X. Kong, M. C. Kelley, J. A. Sosman, D. B. Johnson, A. Ribas, R. S. Lo, Genomic and transcriptomic features of response to anti-PD-1 therapy in metastatic melanoma. *Cell* **165**, 35–44 (2016).
26. J. M. Taube, R. A. Anders, G. D. Young, H. Xu, R. Sharma, T. L. McMiller, S. Chen, A. P. Klein, D. M. Pardoll, S. L. Topalian, L. Chen, Colocalization of inflammatory response with B7-h1 expression in human melanocytic lesions supports an adaptive resistance mechanism of immune escape. *Sci. Transl. Med.* **4**, 127ra137 (2012).
27. J. M. Taube, G. D. Young, T. L. McMiller, S. Chen, J. T. Salas, T. S. Pritchard, H. Xu, A. K. Meeker, J. Fan, C. Cheadle, A. E. Berger, D. M. Pardoll, S. L. Topalian, Differential expression of immune-regulatory genes associated with PD-L1 display in melanoma: Implications for PD-1 pathway blockade. *Clin. Cancer Res.* **21**, 3969–3976 (2015).
28. M. D. Ayers, M. Nebozhyn, H. A. Hirsch, R. Cristescu, E. E. Murphy, S. P. Kang, S. W. Ebbinghaus, T. K. McClanahan, A. Loboda, J. K. Lunceford, Assessment of gene expression in peripheral blood from patients with advanced melanoma using RNA-seq before and after treatment with anti-PD-1 therapy with pembrolizumab (MK-3475). *Cancer Res.* **75**, 1307 (2015).
29. A. J. Minn, E. J. Wherry, Combination cancer therapies with immune checkpoint blockade: Convergence on interferon signaling. *Cell* **165**, 272–275 (2016).
30. J. M. Zaretsky, A. Garcia-Diaz, D. S. Shin, H. Escuin-Ordinas, W. Hugo, S. Hu-Lieskovan, D. Y. Torrejon, G. Abril-Rodriguez, S. Sandoval, L. Barthly, J. Saco, B. Homet Moreno, R. Mezzadra, B. Chmielowski, K. Ruchalski, I. P. Shintaku, P. J. Sanchez, C. Puig-Saus, G. Cherry, E. Seja, X. Kong, J. Pang, B. Berent-Maoz, B. Comin-Anduix, T. G. Graeber, P. C. Tumeh, T. N. Schumacher, R. S. Lo, A. Ribas, Mutations associated with acquired resistance to PD-1 blockade in melanoma. *N. Engl. J. Med.* **375**, 819–829 (2016).
31. H. Matsushita, M. D. Vesely, D. C. Koboldt, C. G. Rickert, R. Uppaluri, V. J. Magrini, C. D. Arthur, J. M. White, Y.-S. Chen, L. K. Shea, J. Hundal, M. C. Wendl, R. Demeter, T. Wylie, J. P. Allison, M. J. Smyth, L. J. Old, E. R. Mardis, R. D. Schreiber, Cancer exome analysis reveals a T-cell-dependent mechanism of cancer immunoediting. *Nature* **482**, 400–404 (2012).
32. M. DuPage, C. Mazumdar, L. M. Schmidt, A. F. Cheung, T. Jacks, Expression of tumour-specific antigens underlies cancer immunoediting. *Nature* **482**, 405–409 (2012).
33. A. Sivan, L. Corrales, N. Hubert, J. B. Williams, K. Aquino-Michaels, Z. M. Earley, F. W. Benyamin, Y. M. Lei, B. Jabri, M.-L. Alegre, E. B. Chang, T. F. Gajewski, Commensal *Bifidobacterium* promotes antitumor immunity and facilitates anti–PD-L1 efficacy. *Science* **350**, 1084–1089 (2015).
34. M. Vétizou, J. M. Pitt, R. Daillère, P. Lepage, N. Waldschmitt, C. Flament, S. Rusakiewicz, B. Routy, M. P. Roberti, C. P. M. Duong, V. Poirier-Colame, A. Roux, S. Becharef, S. Formenti, E. Golden, S. Cording, G. Eberl, A. Schlitzer, F. Ginhoux, S. Mani, T. Yamazaki, N. Jacquelot, D. P. Enot, M. Bérard, J. Nigou, P. Opolon, A. Eggermont, P.-L. Woerther, E. Chachaty, N. Chaput, C. Robert, C. Mateus, G. Kroemer, D. Raoult, I. Gomperts Boneca, F. Carbonnel, M. Chamaillard, L. Zitvogel, Anticancer immunotherapy by CTLA-4 blockade relies on the gut microbiota. *Science* **350**, 1079–1084 (2015).
35. C.-H. Chang, J. Qiu, D. O'Sullivan, M. D. Buck, T. Noguchi, J. D. Curtis, Q. Chen, M. Gindin, M. M. Gubin, G. J. W. van der Windt, E. Tonc, R. D. Schreiber, E. J. Pearce, E. L. Pearce, Metabolic competition in the tumor microenvironment is a driver of cancer progression. *Cell* **162**, 1229–1241 (2015).
36. P.-C. Ho, J. D. Bihuniak, A. N. Macintyre, M. Staron, X. Liu, R. Amezquita, Y.-C. Tsui, G. Cui, G. Micevic, J. C. Perales, S. H. Kleinstein, E. D. Abel, K. L. Insogna, S. Feske, J. W. Locasale, M. W. Bosenberg, J. C. Rathmell, S. M. Kaech, Phosphoenolpyruvate is a metabolic checkpoint of anti-tumor t cell responses. *Cell* **162**, 1217–1228 (2015).
37. W. Yang, Y. Bai, Y. Xiong, J. Zhang, S. Chen, X. Zheng, X. Meng, L. Li, J. Wang, C. Xu, C. Yan, L. Wang, C. C. Y. Chang, T.-Y. Chang, T. Zhang, P. Zhou, B.-L. Song, W. Liu, S.-c. Sun, X. Liu, B.-l. Li, C. Xu, Potentiating the antitumour response of $CD8^+$ T cells by modulating cholesterol metabolism. *Nature* **531**, 651–655 (2016).
38. P.-L. Chen, W. Roh, A. Reuben, Z. A. Cooper, C. N. Spencer, P. A. Prieto, J. P. Miller, R. L. Bassett, V. Gopalakrishnan, K. Wani, M. P. De Macedo, J. L. Austin-Breneman, H. Jiang, Q. Chang, S. M. Reddy, W.-S. Chen, M. T. Tetzlaff, R. J. Broaddus, M. A. Davies, J. E. Gershenwald, L. Haydu, A. J. Lazar, S. P. Patel, P. Hwu, W.-J. Hwu, A. Diab, I. C. Glitza, S. E. Woodman, L. M. Vence, I. I. Wistuba, R. N. Amaria, L. N. Kwong, V. Prieto, R. E. Davis, W. Ma, W. W. Overwijk, A. H. Sharpe, J. Hu, P. A. Futreal, J. Blando, P. Sharma, J. P. Allison, L. Chin, J. A. Wargo, Analysis of immune signatures in longitudinal tumor samples yields insight into biomarkers of response and mechanisms of resistance to immune checkpoint blockade. *Cancer Discov.* **6**, 827–837 (2016).
39. E. Hodis, I. R. Watson, G. V. Kryukov, S. T. Arold, M. Imielinski, J.-P. Theurillat, E. Nickerson, D. Auclair, L. Li, C. Place, D. Dicara, A. H. Ramos, M. S. Lawrence, K. Cibulskis, A. Sivachenko, D. Voet, G. Saksena, N. Stransky, R. C. Onofrio, W. Winckler, K. Ardlie, N. Wagle, J. Wargo, K. Chong, D. L. Morton, K. Stemke-Hale, G. Chen, M. Noble, M. Meyerson, J. E. Ladbury, M. A. Davies, J. E. Gershenwald, S. N. Wagner, D. S. B. Hoon, D. Schadendorf, E. S. Lander, S. B. Gabriel, G. Getz, L. A. Garraway, L. Chin, A landscape of driver mutations in melanoma. *Cell* **150**, 251–263 (2012).
40. Cancer Genome Atlas Network, Genomic classification of cutaneous melanoma. *Cell* **161**, 1681–1696 (2015).
41. D. H. Kaplan, V. Shankaran, A. S. Dighe, E. Stockert, M. Aguet, L. J. Old, R. D. Schreiber, Demonstration of an interferon γ-dependent tumor surveillance system in immunocompetent mice. *Proc. Natl. Acad. Sci. U.S.A.* **95**, 7556–7561 (1998).
42. G. P. Dunn, K. C. F. Sheehan, L. J. Old, R. D. Schreiber, IFN unresponsiveness in LNCaP cells due to the lack of *JAK1* gene expression. *Cancer Res.* **65**, 3447–3453 (2005).
43. J. Gao, L. Z. Shi, H. Zhao, J. Chen, L. Xiong, Q. He, T. Chen, J. Roszik, C. Bernatchez, S. E. Woodman, P.-L. Chen, P. Hwu, J. P. Allison, A. Futreal, J. A. Wargo, P. Sharma, Loss of IFN-γ pathway genes in tumor cells as a mechanism of resistance to anti-CTLA-4 therapy. *Cell* **167**, 397–404.e9 (2016).
44. S. A. Shukla, M. S. Rooney, M. Rajasagi, G. Tiao, P. M. Dixon, M. S. Lawrence, J. Stevens, W. J. Lane, J. L. Dellagatta, S. Steelman, C. Sougnez, K. Cibulskis, A. Kiezun, N. Hacohen, V. Brusic, C. J. Wu, G. Getz, Comprehensive analysis of cancer-associated somatic mutations in class I HLA genes. *Nat. Biotechnol.* **33**, 1152–1158 (2015).
45. E. Wang, A. Worschech, F. M. Marincola, The immunologic constant of rejection. *Trends Immunol.* **29**, 256–262 (2008).
46. J. Galon, H. K. Angell, D. Bedognetti, F. M. Marincola, The continuum of cancer immunosurveillance: Prognostic, predictive, and mechanistic signatures. *Immunity* **39**, 11–26 (2013).
47. L. N. Kwong, L. Chin, Chromosome 10, frequently lost in human melanoma, encodes multiple tumor-suppressive functions. *Cancer Res.* **74**, 1814–1821 (2014).
48. K. Yoshihara, M. Shahmoradgoli, E. Martínez, R. Vegesna, H. Kim, W. Torres-Garcia, V. Treviño, H. Shen, P. W. Laird, D. A. Levine, S. L. Carter, G. Getz, K. Stemke-Hale, G. B. Mills, R. G. W. Verhaak, Inferring tumour purity and stromal and immune cell admixture from expression data. *Nat. Commun.* **4**, 2612 (2013).
49. V. K. Mootha, C. M. Lindgren, K.-F. Eriksson, A. Subramanian, S. Sihag, J. Lehar, P. Puigserver, E. Carlsson, M. Ridderstråle, E. Laurila, N. Houstis, M. J. Daly, N. Patterson, J. P. Mesirov, T. R. Golub, P. Tamayo, B. Spiegelman, E. S. Lander, J. N. Hirschhorn, D. Altshuler, L. C. Groop, PGC-1α-responsive genes involved in oxidative phosphorylation are coordinately downregulated in human diabetes. *Nat. Genet.* **34**, 267–273 (2003).
50. B. C. Bastian, P. E. LeBoit, H. Hamm, E.-B. Bröcker, D. Pinkel, Chromosomal gains and losses in primary cutaneous melanomas detected by comparative genomic hybridization. *Cancer Res.* **58**, 2170–2175 (1998).
51. J. Bauer, B. C. Bastian, Distinguishing melanocytic nevi from melanoma by DNA copy number changes: Comparative genomic hybridization as a research and diagnostic tool. *Dermatol. Ther.* **19**, 40–49 (2006).
52. A. H. Shain, I. Yeh, I. Kovalyshyn, A. Sriharan, E. Talevich, A. Gagnon, R. Dummer, J. North, L. Pincus, B. Ruben, W. Rickaby, C. D'Arrigo, A. Robson, B. C. Bastian, The genetic evolution of melanoma from precursor lesions. *N. Engl. J. Med.* **373**, 1926–1936 (2015).

53. A.H. Shain, B. C. Bastian, From melanocytes to melanomas. *Nat. Rev. Cancer* **16**, 345–358 (2016).
54. H. Li, R. Durbin, Fast and accurate short read alignment with Burrows–Wheeler transform. *Bioinformatics* **25**, 1754–1760 (2009).
55. A. McKenna, M. Hanna, E. Banks, A. Sivachenko, K. Cibulskis, A. Kernytsky, K. Garimella, D. Altshuler, S. Gabriel, M. Daly, M. A. DePristo, The genome analysis toolkit: A MapReduce framework for analyzing next-generation DNA sequencing data. *Genome Res.* **20**, 1297–1303 (2010).
56. M. A. DePristo, E. Banks, R. Poplin, K. V. Garimella, J. R. Maguire, C. Hartl, A. A. Philippakis, G. del Angel, M. A. Rivas, M. Hanna, A. McKenna, T. J. Fennell, A. M. Kernytsky, A. Y. Sivachenko, K. Cibulskis, S. B. Gabriel, D. Altshuler, M. J. Daly, A framework for variation discovery and genotyping using next-generation DNA sequencing data. *Nat. Genet.* **43**, 491–498 (2011).
57. G. A. Van der Auwera, M. O. Carneiro, C. Hartl, R. Poplin, G. del Angel, A. Levy-Moonshine, T. Jordan, K. Shakir, D. Roazen, J. Thibault, E. Banks, K. V. Garimella, D. Altshuler, S. Gabriel, M. A. DePristo, From FastQ data to high-confidence variant calls: The genome analysis toolkit best practices pipeline. *Curr. Protoc. Bioinformatics* **43**, 11.10.1–11.10.33 (2013).
58. K. Cibulskis, M. S. Lawrence, S. L. Carter, A. Sivachenko, D. Jaffe, C. Sougnez, S. Gabriel, M. Meyerson, E. S. Lander, G. Getz, Sensitive detection of somatic point mutations in impure and heterogeneous cancer samples. *Nat. Biotechnol.* **31**, 213–219 (2013).
59. K. Ye, M. H. Schulz, Q. Long, R. Apweiler, Z. Ning, Pindel: A pattern growth approach to detect break points of large deletions and medium sized insertions from paired-end short reads. *Bioinformatics* **25**, 2865–2871 (2009).
60. N. Andor, J. V. Harness, S. Müller, H. W. Mewes, C. Petritsch, EXPANDS: Expanding ploidy and allele frequency on nested subpopulations. *Bioinformatics* **30**, 50–60 (2014).
61. C. A. Miller, B. S. White, N. D. Dees, M. Griffith, J. S. Welch, O. L. Griffith, R. Vij, M. H. Tomasson, T. A. Graubert, M. J. Walter, M. J. Ellis, W. Schierding, J. F. DiPersio, T. J. Ley, E. R. Mardis, R. K. Wilson, L. Ding, SciClone: Inferring clonal architecture and tracking the spatial and temporal patterns of tumor evolution. *PLOS Comput. Biol.* **10**, e1003665 (2014).
62. A. Snyder, T. A. Chan, Immunogenic peptide discovery in cancer genomes. *Curr. Opin. Genet. Dev.* **30**, 7–16 (2015).
63. C. Liu, X. Yang, B. Duffy, T. Mohanakumar, R. D. Mitra, M. C. Zody, J. D. Pfeifer, ATHLATES: Accurate typing of human leukocyte antigen through exome sequencing. *Nucleic Acids Res.* **41**, e142 (2013).
64. I. Hoof, B. Peters, J. Sidney, L. E. Pedersen, A. Sette, O. Lund, S. Buus, M. Nielsen, NetMHCpan, a method for MHC class I binding prediction beyond humans. *Immunogenetics* **61**, 1–13 (2009).
65. F. Favero, T. Joshi, A. M. Marquard, N. J. Birkbak, M. Krzystanek, Q. Li, Z. Szallasi, A. C. Eklund, Sequenza: Allele-specific copy number and mutation profiles from tumor sequencing data. *Ann. Oncol.* **26**, 64–70 (2015).
66. J. Zhang, "CNTools: Convert segment data into a region by sample matrix to allow for other high level computational analyses. R package version 1.6. 0" (2014); https://rdrr.io/bioc/CNTools/.
67. J. Zhang, B. Feng, "biocViews microarray. Package 'cghMCR'" (2013); www.bioconductor.org/packages/release/bioc/html/cghMCR.html.
68. S. A. Forbes, D. Beare, P. Gunasekaran, K. Leung, N. Bindal, H. Boutselakis, M. Ding, S. Bamford, C. Cole, S. Ward, C. Y. Kok, M. Jia, T. De, J. W. Teague, M. R. Stratton, U. McDermott, P. J. Campbell, COSMIC: Exploring the world's knowledge of somatic mutations in human cancer. *Nucleic Acids Res.* **43**, D805–D811 (2015).
69. M. Zhao, J. Sun, Z. Zhao, TSGene: A web resource for tumor suppressor genes. *Nucleic Acids Res.* **41**, D970–D976 (2013).
70. H. S. Robins, P. V. Campregher, S. K. Srivastava, A. Wacher, C. J. Turtle, O. Kahsai, S. R. Riddell, E. H. Warren, C. S. Carlson, Comprehensive assessment of T-cell receptor β-chain diversity in αβ T cells. *Blood* **114**, 4099–4107 (2009).
71. C. S. Carlson, R. O. Emerson, A. M. Sherwood, C. Desmarais, M.-W. Chung, J. M. Parsons, M. S. Steen, M. A. LaMadrid-Herrmannsfeldt, D. W. Williamson, R. J. Livingston, D. Wu, B. L. Wood, M. J. Rieder, H. Robins, Using synthetic templates to design an unbiased multiplex PCR assay. *Nat. Commun.* **4**, 2680 (2013).

Funding: J.A.W. acknowledges the Melanoma Research Alliance Team Science Award, the Kenedy Memorial Foundation grant #0727030, U54CA163125, the Rising STARs (Science and Technology Acquisition and Retention) award of the University of Texas System Board of Regents, Regents' Health Research Scholar Award of the University of Texas System Board of Regents, and the generous philanthropic support of several families whose lives have been affected by melanoma. This work was supported by NIH grants 1K08CA160692-01A1 (to J.A.W.), U54CA163125 (to Z.A.C., J.A.W., and L.C.), T32CA009599 (to P.A.P.), T32CA163185 (to P.-L.C. and W.-S.C.), NIH T32 CA009666 (to S.M.R.), and R01 CA187076-02 (to M.A.D. and P.H.). J.P.A., P.S., and J.A.W. are members of the Parker Institute for Cancer Immunotherapy at the MD Anderson Cancer Center. W.R. was supported by the Cancer Prevention Research Institute of Texas (CPRIT) Graduate Scholar Award. I.C.G. holds a Conquer Cancer Foundation of American Society of Clinical Oncology Young Investigator Award. L.C. is a CPRIT Scholar in Cancer Research and was supported by a grant from the CPRIT (R1204). P.A.F. holds CPRIT funding (R1205 01), a Robert Welch Distinguished University Chair (G-0040), and STARs (Science and Technology Acquisition and Retention) award of the University of Texas System Board of Regents. R.N.A. has received research support from Merck, Novartis/Array, and Bristol-Myers Squibb. W.-J.H. has received research support from Bristol-Myers Squibb, Merck, GlaxoSmithKline (GSK), and MedImmune. This work was supported by MD Anderson's Institutional Tissue Bank Award (2P30CA016672) from the National Cancer Institute. This study was also supported by philanthropic contributions to the UT MD Anderson Cancer Center Melanoma Moon Shot Program and the Dr. Miriam and Sheldon G. Adelson Medical Research Foundation. **Author contributions:** W.R., P.-L.C., Z.A.C., P.S., J.P.A., L.C., J.A.W., and P.A.F. designed the experiments. W.R., P.-L.C., A.R., J.A.W., and P.A.F. wrote the manuscript. All authors edited the manuscript. W.R., P.-L.C., A.R., J.R., J.P.M., Z.A.C., J.A.W., and P.A.F. analyzed the data. W.R., J.R., F.W., and J.Z. ran the computational pipelines. W.R. and J.H. performed the statistical analyses. P.-L.C., C.N.S., P.A.P., V.G., M.A.D., J.E.G., P.H., S.P.P., A.D., I.C.G., H.T., W.-J.H., S.E.W., R.N.A., and J.A.W. acquired and compiled the clinical and response data. C.N.S., P.-L.C., M.T.T., M.A.D., J.E.G., S.P.P., A.D., I.C.G., H.T., A.J.L., P.H., W.-J.H., S.E.W., R.N.A., V.G.P., and J.A.W. enrolled the subjects and contributed the samples. P.-L.C., W.-S.C., and M.T.T. performed the pathological assessment. P.-L.C., J.P.M., C.G., S.M.R., L.L., Q.C., K.W., M.P.D.M., E.C., W.-S.C., J.L.A.-B., and H.J. performed the experiments. J.A.W. and P.A.F. supervised the study. **Competing interests:** J.A.W. has honoraria from speakers' bureau of Dava Oncology, Illumina and is an advisory board member for GSK, Roche/Genentech, Novartis, and Bristol-Myers Squibb. M.A.D. is an advisory board member for GSK, Roche/Genentech, Novartis, and Sanofi-Aventis and has received research support from GSK, Roche/Genentech, Sanofi-Aventis, Oncothyreon, Myriad, and AstraZeneca. J.E.G. is on the advisory board of Merck and receives royalties from Mercator Therapeutics. S.P.P. has honoraria from speakers' bureau of Dava Oncology, Bristol-Myers Squibb, and Merck and is an advisory board member for Amgen and Roche/Genentech. P.H. serves on the advisory board of Lion Biotechnologies and Immatics US. W.-J.H. serves on the advisory board of Merck's melanoma advisory board. R.N.A. has received research support from Merck, Novartis, and Bristol-Myers Squibb. P.S. is a consultant for Bristol-Myers Squibb, Jounce Therapeutics, Helsinn, and GSK as well as a stockholder from Jounce Therapeutics. J.P.A. is a consultant and stockholder for Jounce Therapeutics, receives royalties from Bristol-Myers Squibb, and has intellectual property with Bristol-Myers Squibb and Merck. Z.A.C. is an employee in MedImmune and owns stock or options in AstraZeneca. The other authors declare that they have no competing interests. **Data and materials availability:** WES data (BAM files) from melanoma patients from our cohort are available at dbGaP (BioProject ID: PRJNA369259). WES data (SAM files) and RNA-seq data (FASTQ files) from melanoma patients from the Van Allen cohort are available at dbGaP (accession number phs000452.v2.p1).

Submitted 3 August 2016
Resubmitted 17 November 2016
Accepted 4 February 2017
Published 1 March 2017
10.1126/scitranslmed.aah3560

Citation: W. Roh, P.-L. Chen, A. Reuben, C. N. Spencer, P. A. Prieto, J. P. Miller, V. Gopalakrishnan, F. Wang, Z. A. Cooper, S. M. Reddy, C. Gumbs, L. Little, Q. Chang, W.-S. Chen, K. Wani, M. P. De Macedo, E. Chen, J. L. Austin-Breneman, H. Jiang, J. Roszik, M. T. Tetzlaff, M. A. Davies, J. E. Gershenwald, H. Tawbi, A. J. Lazar, P. Hwu, W.-J. Hwu, A. Diab, I. C. Glitza, S. P. Patel, S. E. Woodman, R. N. Amaria, V. G. Prieto, J. Hu, P. Sharma, J. P. Allison, L. Chin, J. Zhang, J. A. Wargo, P. A. Futreal, Integrated molecular analysis of tumor biopsies on sequential CTLA-4 and PD-1 blockade reveals markers of response and resistance. *Sci. Transl. Med.* **9**, eaah3560 (2017).

Science Translational Medicine

Integrated molecular analysis of tumor biopsies on sequential CTLA-4 and PD-1 blockade reveals markers of response and resistance

Whijae Roh, Pei-Ling Chen, Alexandre Reuben, Christine N. Spencer, Peter A. Prieto, John P. Miller, Vancheswaran Gopalakrishnan, Feng Wang, Zachary A. Cooper, Sangeetha M. Reddy, Curtis Gumbs, Latasha Little, Qing Chang, Wei-Shen Chen, Khalida Wani, Mariana Petaccia De Macedo, Eveline Chen, Jacob L. Austin-Breneman, Hong Jiang, Jason Roszik, Michael T. Tetzlaff, Michael A. Davies, Jeffrey E. Gershenwald, Hussein Tawbi, Alexander J. Lazar, Patrick Hwu, Wen-Jen Hwu, Adi Diab, Isabella C. Glitza, Sapna P. Patel, Scott E. Woodman, Rodabe N. Amaria, Victor G. Prieto, Jianhua Hu, Padmanee Sharma, James P. Allison, Lynda Chin, Jianhua Zhang, Jennifer A. Wargo and P. Andrew Futreal

Sci Transl Med **9**, eaah3560.
DOI: 10.1126/scitranslmed.aah3560

Checking on checkpoint inhibitors

Immune checkpoint blockade has greatly improved the success of treatment in melanoma and other tumor types, but it is expensive and does not work for all patients. To optimize the likelihood of therapeutic success and reduce the risks and expense of unnecessary treatment, it would be helpful to find biomarkers that can predict treatment response. Roh *et al.* studied patients treated with sequential checkpoint inhibitors targeting CTLA-4 and then PD-1. In these patients, the authors discovered that a more clonal T cell population specifically correlates with response to PD-1 blockade, but not CTLA-4, which may help identify the best candidates for this treatment. In addition, increased frequency of gene copy number loss was correlated with decreased responsiveness to either therapy.

Science Translational Medicine (ISSN 1946-6242) is published by the American Association for the Advancement of Science, 1200 New York Avenue NW, Washington, DC 20005. The title *Science Translational Medicine* is a registered trademark of AAAS.